Multi-source remote sensing image matching based on contourlet transform and Tsallis entropy

WU Yiquan, CHEN Sa

School of Information Science and Technology, Nanjing University of Aeronautics and Astronautics, Jiangsu Nanjing 210016, *China*

Abstract: There are a lot of differences in multi-source remote sensing images from various sensors about the same scene. Maximization of mutual information can be used for the multi-source image matching, but the accuracy and efficiency of image matching need to be further improved. Therefore, an algorithm for multi-source remote sensing image matching was proposed in this paper, based on contourlet transform, Tsallis entropy based mutual information and improved particle swarm optimization. Firstly, the target image and reference image were decomposed to the low resolution image using contourlet transform, respectively. Then, a new image similarity measure criterion, the Tsallis entropy based mutual information, was used to achieve the global optimization. Meanwhile, a modified extremum disturbed and simple particle swarm optimization algorithm was applied to match the lowest resolution remote sensing images. Based on the preliminary result, the matching between the higher resolution images could be implemented stepwise up to the full resolution images. The experimental results show that, compared with those of other existing remote sensing image matching methods, the proposed algorithm has the high accuracy, strong robustness and requires much fewer operations.

Key words: multi-source remote sensing image matching, contourlet transform, Tsallis entropy, particle swarm optimization

CLC number: TP751.1 **Document code:** A

Citation format: Wu Y Q, Chen S. 2010. Multi-source remote sensing image matching based on contourlet transform and Tsallis entropy. *Journal of Remote Sensing*. **14**(5): 893—904

1 INTRODUCTION

Image matching, one of the key technologies in image understanding and computer vision, has a wide application prospect in many fields, such as the vehicle cruise guidance, moving object tracking and recognition, aerial photogrammetry, video motion estimation, image retrieval and so on. In remote sensing image processing, image matching technology is applied to positioning and registration (Brown, 1992; Barbara & Jan, 2003; Zhang *et al*., 2005; Li *et al*., 2006). The region in reference image which corresponds to target image is determined by calculating the similarity. Usually, image matching methods are divided into two categories, pixel-based matching and feature-based matching. Due to the different imaging principles of multi-source remote sensors, the gray scale gap among the images of the same scene becomes large. If using the normalized cross-correlation which has high requirement on gray correlation, the matching result can hardly be satisfied, and is vulnerable to noise. If using the feature-based matching algorithm by exacting the image edges, it will generate matching errors, or even can not match for homogenous region, such as water area, because of the inconsistent edges and contours.

Since 1994, mutual information measure criterion has been used in medical image registration, and has received a wide range of research and application. It doesn't need to make any assumption about the relationship of image gray scale. No pretreatment is required. Because of the high precision and strong robustness, mutual information measure criterion is suitable for multi-modal image matching, and therefore it is considered to apply to multi-source remote sensing image matching. Cole-Rhodes *et al*. (2003) introduced a multi-resolution registration of remote sensing imagery by optimization of mutual information using a stochastic gradient. The experimental results show that mutual information is more suitable than cross-correlation for multi-source image matching. Tian *et al*. (2006) adopted the similarity of regional mutual information in matching algorithm, to solve the issue of weak correlation among the gray spectrum. However, when applying mutual information to image matching, the precision needs to be further improved. Furthermore, estimation of mutual information, which is iteratively required, is a time-consuming process.

In view of the matching precision, Tsallis entropy (Martin *et al*., 2001; Furuichi, 2006; Waleed & Ben, 2009) based mutual information is considered to solve the problem. The system

Received: 2009-07-23; **Accepted**: 2009-11-09

Foundation: National Natural Science Foundation of China (No.60872065).

First author biography: WU Yiquan (1963—), male, Ph.D, professor, graduated from Nanjing University of Aeronautics and Astronautics, majoring in Information and Communication Engineering. His main research includes image processing, analysis and understanding, target detection and tracking, and signal processing. He has already published more than 80 academic papers in core periodicals and collections of international conference. E-mail: nuaaimage @yahoo.com.cn

description of conventional Shannon entropy is extensive, yet practical systems have time and space correlation more or less, which are nonextensive. As a result, Tsallis proposed nonextensive entropy, namely Tsallis entropy, which is more universal, accurate and effective than Shannon entropy. According to this, we use Tsallis entropy based mutual information as similarity measure criterion, to further improve the matching precision, instead of conventional mutual information based on Shannon entropy.

Aiming at the operation efficiency, improved algorithms have been proposed in succession recently. Some (You & Bhattacharya, 2001; Yamamura *et al*., 2007) reduced the computation load through compressing searching space, for example, multi-resolution structure based on wavelet transform was used to match from coarse to fine. Some (Prachya *et al*., 2001; Xu *et al*., 2005; Yang & Zhang, 2006; Zhang *et al*., 2008) accelerated the matching speed by various optimization algorithms, and one of the most typical methods was genetic algorithm (GA), which was a non-ergodic optimization search strategy. Contourlet transform, proposed in recent years (Donoho & Vetterli, 2005), has the characteristics of multi-resolution, localization, critical sampling, directionality and anisotropy. Thus, we can use these characteristics in image matching, especially multi-resolution. As for the latter, basic genetic algorithm has poor ability of local optimization, and parameters have a great impact on the results. Particle swarm optimization (PSO) achieves swarm intelligence optimal search by studying and updating (Sjahputera & Keller, 2005; Li & Ji, 2007). Compared with genetic algorithm, PSO is simple and easy to implement, and is a highly efficient parallel search algorithm which needs less adjustable parameters. Therefore, it is expected to reduce the computation time significantly.

Taken together, a multi-source remote sensing image matching algorithm based on contourlet transform, Tsallis entropy and improved particle swarm optimization was introduced. The algorithm mainly contains the following aspects: (1) Decompose the target image and reference image to low resolution with contourlet transform, respectively. Match the lowest resolution remote sensing images. Based on the preliminary result, the matching between the higher resolution images can be implemented stepwise up to the full resolution images. (2) For two same size images, target image and the sub-reference image, use Tsallis entropy based mutual information as similarity measure criterion to advance the matching precision. (3) Apply a modified extremum disturbed and simple particle swarm optimization algorithm (mtsPSO) to image matching, so that the operation speed can be further improved.

2 PRINCIPLE OF CONTOURLET TRANSFORM, PSO AND MUTUAL INFORMATION

2.1 Contourlet transform

Discrete Contourlet transform, also called Pyramidal Direction Filter Bank (PDFB), mainly has two stages: subband decomposition and directional transform. The Laplacian Pyramid is first to capture the point discontinuities, and then followed by a directional filter bank to link point discontinuities into a coefficient. Fig.1 shows the decomposition scheme of contourlet transform. The original image is decomposed into a lowpass image and several high frequency components, which distributed on multiple scales and multiple directions.

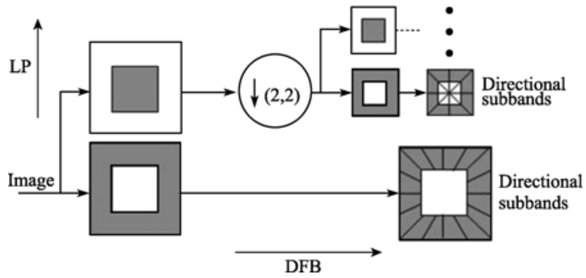

Fig. 1 Contourlet filter bank

2.2 Basic particle swarm optimization algorithm

For an n-dimensional search space, the position and velocity of the i-th particle are represented as $\boldsymbol{X}_i=(X_{i1},X_{i2},\cdots,X_{in})$ and $\boldsymbol{V}_i=(V_{i1},V_{i2},\cdots,V_{in})$, respectively. The former stands for the solution of the problem, and corresponds to the objective function value which is used to evaluate the fitness of particles. The latter denotes the new velocity of a particle from the current position to its next position. At first, initialize the particle swarm; and then search for the optimal solution by iterating. Suppose that, in the t-th iteration, $\boldsymbol{p}_i(t)$ is the best previous position of the i-th particle, named individual extremum; $\boldsymbol{g}(t)$ is the best previous position discovered by the whole swarm, named global extremum. In the $(t+1)$-th iteration, the particles are manipulated according to the following equations:

$$\begin{aligned}\boldsymbol{V}_i(t+1) = w\boldsymbol{V}_i(t) + c_1r_1\left[\boldsymbol{p}_i(t) - \boldsymbol{X}_i(t)\right] + \\ c_2r_2\left[\boldsymbol{g}(t) - \boldsymbol{X}_i(t)\right]\end{aligned} \tag{1}$$

$$\boldsymbol{X}_i(t+1) = \boldsymbol{X}_i(t) + \boldsymbol{V}_i(t+1) \tag{2}$$

where c_1 and c_2 are two acceleration constants that regulate the relative velocities with respect to the best global and local positions, respectively. In this paper, $c_1=c_2=2$; r_1 and r_2 are random variables drawn from a uniform distribution in the range (0,1); w is the weight coefficients, which is usually reduces linearly as interaction time:

$$w = w_{\max} - t \times \frac{w_{\max} - w_{\min}}{t_{\max}} \tag{3}$$

where $w_{\max}$ and $w_{\min}$ denote the maximum and minimum inertia weight, respectively; $t_{\max}$ stands for the total iteration time. In the iteration update process, the velocity is restricted to the range $V_i\in[V_{\min},V_{\max}]$, the position is limited in permissible range, the final output $\boldsymbol{g}$ is the global optimal solution.

2.3 Shannon entropy based mutual information

Mutual information usually describes the statistical correlation between two systems, which can be expressed by entropy. Shannon entropy of system A is defined as,

$$H(A) = -\sum_{a} p_A(a)\log p_A(a) \tag{4}$$

The joint entropy of system A and B is given as

$$H(A,B) = -\sum_{a,b} p_{A,B}(a,b)\log p_{A,B}(a,b) \tag{5}$$

where $a\in A$, $b\in B$; $p_A(a)$ denotes the probability density of system A; $p_{A,B}(a,b)$ is the joint probability density of system A and B. If $H(A|B)$ denotes conditional entropy of A, when system B is known. The mutual information of two systems is described as:

$$\begin{aligned} I(A,B) &= H(A)+H(B)-H(A,B) \\ &= H(A)-H(A\,|\,B) \end{aligned} \tag{6}$$

Use generalized distance of probability distribution to estimate the mutual information,

$$I(A,B) = \sum_{a,b} p_{A,B}(a,b)\log\frac{p_{A,B}(a,b)}{p_A(a)p_B(b)} \tag{7}$$

3 REALIZATION PROCESS OF THE PROPOSED ALGORITHM

A novel image matching algorithm for multi-source remote sensing images based on contourlet transform, Tsallis entropy and improved particle swarm optimization is proposed. In the algorithm, images are matched from coarse to fine, using the multi-resolution of contourlet transform; and Tsallis entropy based mutual information is introduced as a new image similarity measure criterion; meanwhile, the mtsPSO is used to overcome the shortcomings of bPSO, such as relapsing into local extremum, slow convergence velocity and low convergence precision in the late evolutionary. The detail realization process of the proposed algorithm is as following:

(1) The target image and reference image are decomposed by contourlet transform. Where, we use “9-7” pyramid filter, since the linear phase and approximate orthogonality make it more suitable for image signal processing. We choose “pkva” directional filter, and the number of directional subbands in each scale is 4. The decomposition levels are determined by target image, and the low resolution image shouldn’t be too small, or it will generate matching errors for too little information it contains. In this paper, L=2.

(2) Initialize the particle swarm in the low resolution of reference image: Generate random positions of m particles $\boldsymbol{X}$, which is the position offset of target image relative to reference image (Δx, Δy). Set $\boldsymbol{p}$ as the current position of each particle, and $\boldsymbol{g}$ as any of $\boldsymbol{p}$. Set parameters: $t_{\max}$=500, t=0, m=50.

(3) Calculate the fitness function. For target image A and the subimage of reference image B which is as the same size as target image. Use Tsallis entropy based mutual information $I_q(A,B)$ as the fitness function. Evaluate each particle’s fitness F_p according to the position $\boldsymbol{X}$. The derivation is given as following:

For any non-negative real number q and the probability distribution $p(x)$ of the random variable x, Tsallis entropy is defined as,

$$S_q(X) = \frac{1}{q-1}\left[1-\sum_{x} p(x)^q\right] \tag{8}$$

In particular, Tsallis entropy converges to Shannon entropy, as $q\to 1$.

Deprive Tsallis entropy based mutual information as following:

$$\begin{aligned} I_q(A,B) &= S_q(A)-S_q(A\,|\,B) \\ &= S_q(A)+S_q(B)-S_q(A,B) \\ &= S_q(A)+S_q(B)-[S_q(A)+S_q(B)+ \\ &\quad (1-q)S_q(A)S_q(B)] \\ &= (q-1)S_q(A)S_q(B) \end{aligned} \tag{9}$$

Considering Eq.(8) and Eq.(9), we can get

$$\begin{aligned} I_q(A,B) = \frac{1}{|\,q-1\,|}[1-\sum_{a} p(a)-\sum_{b} p(b)+ \\ \sum_{a} p(a)\sum_{b} p(b)] \end{aligned} \tag{10}$$

In the multi-source remote sensing image matching, target image and reference image are taken from different imaging devices, but they are based on the same scene. So when they are perfectly matched, the mutual information of corresponding pixels expressed in one image about the other image must be maximum.

(4) Update individual extremum $\boldsymbol{p}$ and global extremum $\boldsymbol{g}$. If the particle’s fitness is better than that of the current individual extremum, then set $\boldsymbol{p}$ as the particle’s position, and update individual extremum. If the fitness of the best individual extreme of all the particles is better than that of the current global extremum, then set $\boldsymbol{g}$ as the particle’s position, and update global extremum.

(5) Update $\boldsymbol{X}$. The mtsPSO discards the particle velocity and reduces the bPSO from the second order to the first order difference equation. The evolutionary process is only controlled by the variables of the particles position, which avoids the demerits caused by particle velocity, such as relapsing into local extremum, slow convergence velocity and low convergence precision in the late evolutionary. Meanwhile, it accelerates the particles to overstep the local extremum, and improves the practicality of the particle swarm optimization. The update process of the algorithm is given as following:

$$\begin{aligned} \boldsymbol{X}_i(t+1) = w\boldsymbol{X}_i(t)+c_1r_1[r_3^{t_0>T_0}\,\boldsymbol{p}_i-\boldsymbol{X}_i(t)]+ \\ c_2r_2[r_4^{t_g>T_g}\,\boldsymbol{g}-\boldsymbol{X}_i(t)] \end{aligned} \tag{11}$$

where t_0 and t_g stand for the numbers of stagnation steps of individual extremum and global extremum, respectively. T_0 and T_g represent the thresholds of stagnation steps when the individual extremum and global extremum need to be disturbed. $r_3^{t_0>T_0} = \begin{cases} 1 & t_0 \leqslant T_0 \\ U(0,1) & t_0 > T_0 \end{cases}$ and $r_4^{t_g>T_g} = \begin{cases} 1 & t_g \leqslant T_g \\ U(0,1) & t_g > T_g \end{cases}$ are uniform random numbers with condition. $U(0,1)$ denotes random variables drawn from a uniform distribution in the range (0,1). Let T_0=T_g=10.

Considering large inertia weight is benefit to the ability of global search, when small inertia weight is benefit to the ability of local search, mtsPSO proposed in this paper is modified based on the extremum disturbed and simple particle swarm optimization (Hu & Li, 2007). Inertia weights achieve the best balanced inertia factors adaptively, using the strategy of decreasing inertia weight (Chen *et al*., 2006):

$$w = (w_{\text{start}} - w_{\text{end}})\left(\frac{t}{t_{\max}}\right)^2 + (w_{\text{end}} - w_{\text{start}})\left(\frac{2t}{t_{\max}}\right) + w_{\text{start}} \quad (12)$$

In this paper, we set w_{start}=0.95,w_{end}=0.4.

(6) Iteration. Let t=t+1. Check whether it meets the end of the condition: If t=$t_{\max}$ or satisfy the terminating criteria which is problem-dependent, stop iterating and output the best solution, else go to step (3).

(7) According to the position of the best solution $\boldsymbol{g}_L$, the best offset in low resolution image Δx_L、 Δy_L can be determined and output.

(8) In the scale of L−1, continue to search in the neighborhood of point ($2\Delta x_L$, $2\Delta y_L$), and find the best offset position (Δx_{L-1}, Δy_{L-1}) in the current scale. Repeat the process, until the best offset position (Δx_0, Δy_0) in full resolution image is found.

4 EXPERIMENTAL RESULTS AND ANALYSIS

We carried out the experiments on 200 groups of remote sensing images, and chose three of them to illustrate, that were SPOT image (256×256, Fig. 2(a)) and TM image (50×50, Fig.2(b)), visible image (256×256, Fig.2(d)) and SAR image (50×50, Fig.2(e)), visible image (256×256, Fig.2(g)) and infrared image (5×50, Fig.2(h)). The platform used for the experiments was Matlab 7.1 on a PIV-based 2. 78GHz PC with 512M memory. The results are shown in Fig.2(c) (f) (i).

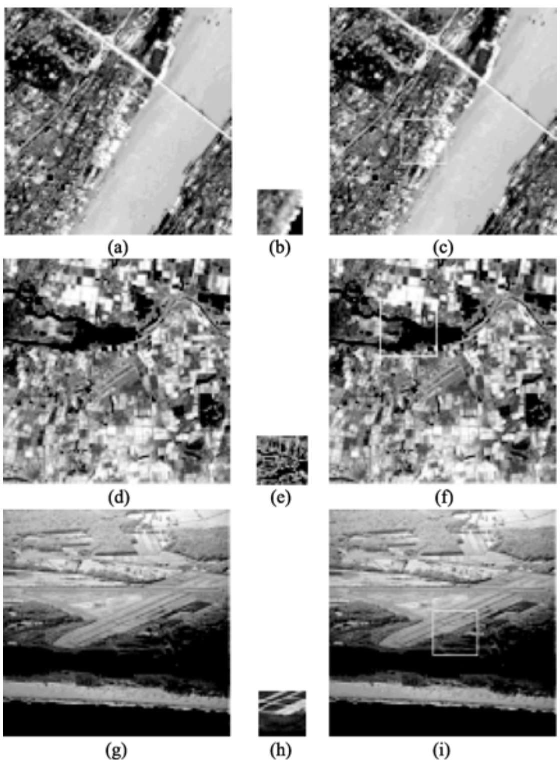

Fig. 2 Images of the three experiments

(a) Reference image of experiment 1; (b) Target image of experiment 1; (c) Result of experiment 1; (d) Reference image of experiment 2; (e) Target image of experiment 2; (f) Result of experiment 2; (g) Reference image of experiment 3; (h) Target image of experiment 3; (i) Result of experiment 3

4.1 Comparison with the experimental results for different decomposition levels *L*

The decomposition level L is determined by target image. Take the experiments on the above images, and run the program 50 times, compute the average values as matching points. The results are shown in Table 1, where point coordinates are subject to the left corner coordinates of matching images.

Table 1 Matching results for different decomposition levels

	L	Matching position	Matching error	Average time/s
Experiment 1	0	(122,80)	(−4, −2)	10.47238
	1	(126,82)	(0,0)	5.99021
	2	(126,82)	(0,0)	3.38824
Experiment 2	0	(37,46)	(0,0)	10.01475
	1	(37,46)	(0,0)	5.78250
	2	(37,46)	(0,0)	3.22392
Experiment 3	0	(114,120)	(−1,2)	10.75026
	1	(115,118)	(0,0)	6.10187
	2	(115,118)	(0,0)	3.40373

Tabel 1 shows that, when L gets smaller, there exists minor matching errors and is quite time-consuming; when L gets larger, fewer operations are needed. However, due to the less information that low resolution image contains, when the number of decomposition levels increases, there will be error matching.

4.2 Comparison with the experimental results of different algorithms

To prove the superiority, we did some contrast experiments using different algorithms, that were: (a) image matching algorithm based on cross correlation and PSO (Sjahputera & Keller, 2005); (b) image matching algorithm based on mutual information and PSO (Li & Ji, 2007); (c) image matching algorithm based on wavelet transform, mutual information and GA (Yang & Zhang, 2006); (d) image matching algorithm based on wavelet transform, mutual information and PSO (Zhang *et al*., 2008); (e) image matching algorithm proposed in this paper, based on contourlet transform, Tsallis entropy based mutual information and mtsPSO. Where L=2, q=0.8, and each program of algorithm run 50 times. Only when matching error equals to (0,0), the solution is correct. The results are shown in Table 2, where correct matching ratio is defined as the number of correct solutions to total operation time ratio.

Since the resolutions of optimization algorithm, such as GA and PSO, have some uncertainty, we executed the programs for multiple times. It is seen that, algorithm (a) can hardly get the

Table 2 Matching results of different algorithms

	Matching algorithm	Average time/s	Correct matching ratio/%
Experiment 1	(a)	4.99721	0
	(b)	50.01207	8
	(c)	19.38394	46
	(d)	14.14857	42
	(e)	3.38824	92
Experiment 2	(a)	4.68990	2
	(b)	50.92149	10
	(c)	19.28786	60
	(d)	14.87391	60
	(e)	3.22392	98
Experiment 3	(a)	4.66313	0
	(b)	50.69498	6
	(c)	18.85430	40
	(d)	14.00925	38
	(e)	3.40373	96

correct matching position. Because of the different imaging principles of multi-source remote sensors, the gray scale gap among the images is large. As a result, the gray linear relationship can not be established and correct matching position can not be found based on cross-correlation. Compared with algorithm (a), algorithm (b) applies mutual information to similarity measure criterion, so that it overcomes the matching errors caused by gray scale to a certain extent. However, the search range is still too large to decrease the computational complexity efficiently. Algorithm (c) and (d) bring in wavelet transform based on algorithm (b), in order to accelerate the search speed while keep the accuracy. Algorithm (c) is more time-consuming than algorithm (c), due to the more steps of GA, such as crossover and mutation. Using contourlet transform, Tsallis entropy based mutual information and mtsPSO, the precision of algorithm (e) is obviously higher than that of other four algorithms, besides it has the best stability and the computation speed is above four times faster than algorithm (b), (c) and (d).

4.3 Anti-noise ability of algorithm

Add Gaussian noise into the given images, whose mean is 0, variance is 0.01. Matching results using the proposed algorithm are shown as Fig.3.

The matching positions are (126, 80), (38, 46) and (115, 118), with the matching errors (0, −2), (1, 0) and (0,0), respectively. The results show that, the proposed algorithm has a certain anti-noise ability. For the noisy images, it can still get accurate solution. It is proved by many experiments that, when target image gets larger, the anti-noise ability gets stronger. That’s because the larger image is, the more information it contains, and the stronger anti-noise ability it has.

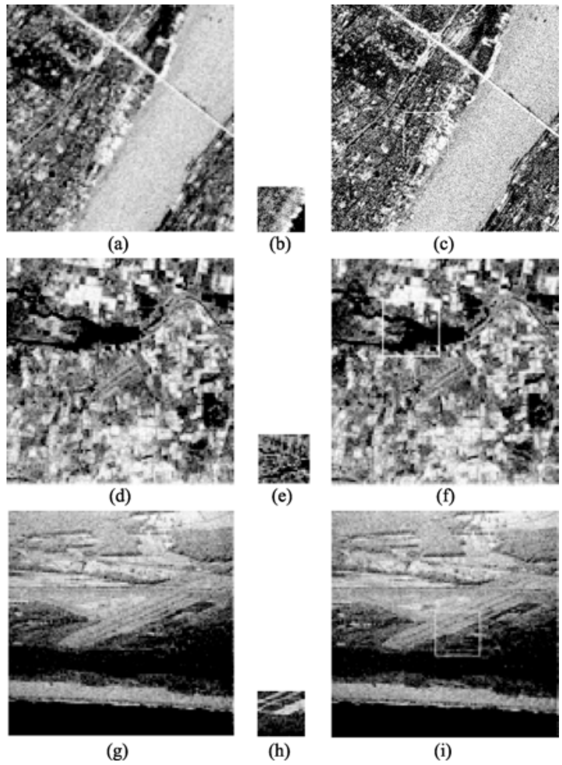

Fig. 3 Noisy images of the three experiments
(a) Reference image of experiment 1; (b) Target image of experiment 1; (c) Result of experiment 1; (d) Reference image of experiment 2; (e) Target image of experiment 2; (f) Result of experiment 2; (g) Reference image of experiment 3; (h) Target image of experiment 3; (i) Result of experiment 3

5 CONCLUSION

An image matching algorithm for multi-source remote sensing images was proposed, based on contourlet transform, Tsallis entropy based mutual information and improved particle swarm optimization. The target image and reference image were firstly decomposed by contourlet transform, and Tsallis entropy based mutual information was applied to similar measure criterion. Meanwhile an extremum disturbed and simple particle swarm optimization algorithm was introduced to match the multi-resolution images from coarse to fine. We analyzed the results through different decomposition levels and different algorithms. The results show that, compared with those of other existing remote sensing image matching methods, the proposed algorithm has high accuracy, strong robustness and requires much fewer operations. Next we consider working on the image matching problem of large angle rotation.

REFERENCES

Barbara Z and Jan F. 2003. Image registration methods: a survey. *Image and Vision Computing*, **21**(11): 977—1000

Brown L G. 1992. A survey of image registration techniques. *ACM Computing Surveys*, **24** (4): 325—376

Chalermwat P, El-Ghazawi T and LeMoigne J. 2001. Two-phase genetic algorithm-based image registration on parallel clusters. *Journal of Future Generation Computing Systems*, **17**: 467—476

Chen G M, Jia J Y and Han Q. 2006. Study on the strategy of decreasing inertia weight in particle swarm optimization algorithm. *Journal of Xi'an Jiaotong University*, **40**(1): 53—56

Cole-Rhodes A A, Johnson K L, Le-Moigne J and Zavorin I. 2003. Multiresolution registration of remote sensing imagery by optimization of mutual information using a stochastic gradient. *Image Processing*, **12**(12): 1495—1511

Donoho M N and Vetterli M. 2005. The contourlet transform: an efficient directional multiresolution image representation. *IEEE Transactions on Image Processing*, **14**(12): 2091—2106

Furuichi S. 2006. Information theoretical properties of tsallis entropies. *Journal of Mathematical Physics*, **47**(2): 23302-1—18

Hu W and Li Z S. 2007. A simpler and more effective particle swarm optimization algorithm. *Journal of Software*, **18**(4): 861—868

Li Q and Ji H B. 2007. Medical image registration based on maximization of mutual information and particle swarm optimization. 5th International Conference on Photonics and Imaging in Biology and Medicine, 6534: 5342—5344

Li X M, Zheng L and Hu Z Y. 2006. SIFT based automatic registration of remotely-sensed imagery. *Journal of Remote Sensing*, **10**(6): 885—892

Martin S, Morison G H, Nailon W H and Durrani. 2001. Fast and accurate image registration using tsallis entropy and simultaneous perturbation stochastic approximation. *IET Electronics Letters*, **40**(10): 595—597

Sjahputera O and Keller JM. 2005. Particle swarm over scene matching. IEEE Swarm Intelligence Symposium

Tian W G, Guo L, Li H H and Yang W L. 2008. A point-based algorithm for multi-spectral image registration using mutual information of regions. *Journal of Optoelectronics Laser*, **19**(6): 799—783

Waleed M and Ben H A. 2009. Nonextensive entropic image registration. *Image Analysis and Recognition*, 5627: 116—125

Xu J B, Hong W and Wu Y R. 2005. The study of remote sensing images matching method based on wavelet transform and genetic algorithms. *Journal of Electronics & Information Technology*, **27**(2): 283—285

Yang F and Zhang H L. 2006. Multiresolution 3-D image registration using hybrid genetic algorithm and powell's method. *Journal of Optoelectronics · Laser*, **17**(6): 26—30

You J and Bhattacharya P A. 2000. Wavelet-based coarse-to-fine image matching scheme in a parallel virtual machine environment. *IEEE Transactions on Image Processing*, **9**(9): 1547—1559

Yutaro Y, Hyoungseop K, Jookooi T, Ishikawa S and Yamaoto A. 2007. A method for reducing of computation time on image registration employing wavelet transformation. International Conference on Control, Guangzhou

Zhang J X, Li G S and Zeng Y. 2005. The study on automatic and high-precision rectification and registration of multi-source remote sensing imagery. *Journal of Remote Sensing*, **9**(1): 73—77

Zhang Q, Yang J and Jia D D. 2008. Image registration based on wavelet transform and hybrid optimization algorithm. *Computer Engineering*, **34**(7): 189—191

Contourlet 变换和 Tsallis 熵的多源遥感图像匹配

吴一全，陈 飒

南京航空航天大学 信息科学与技术学院，江苏 南京 210016

摘 要： 提出了一种利用 Contourlet 变换、Tsallis 熵和改进粒子群优化的多源遥感图像匹配算法。在分别对参考图像和目标图像进行 Contourlet 分解的基础上，以基于 Tsallis 熵的互信息量作为相似性度量准则，利用改进的带极值扰动的简化粒子群优化算法对低分辨率的遥感图像进行匹配操作，逐级上推，最终实现全分辨率情况下多源遥感图像的匹配。实验结果表明，与常用的遥感图像匹配算法相比，该算法匹配精度高，稳健性好，且运算量大幅减少。

关键词： 多源遥感图像匹配, Contourlet 变换, Tsallis 熵，粒子群优化

中图分类号： TP751.1 文献标志码： A

引用格式： 吴一全，陈 飒. 2010. Contourlet 变换和 Tsallis 熵的多源遥感图像匹配. 遥感学报, **14**(5): 893—904

Wu Y Q, Chen S. 2010. Multi-source remote sensing image matching based on contourlet transform and Tsallis entropy. *Journal of Remote Sensing*. **14**(5): 893—904

1 引 言

图像匹配是图像理解和计算机视觉中的关键技术之一，在飞行器巡航制导、运动目标跟踪和识别、航空摄影测量、视频运动估计和图像检索等领域有广阔的应用前景。在遥感图像处理方面，图像匹配技术可以应用于遥感图像的定位和配准(张继贤等, 2005; 李晓明等, 2006; Brown, 1992; Barbara & Jan, 2003)，它通过比较目标图像和参考图像之间的相似性确定目标图像在参考图像中的位置，通常采用基于灰度或基于特征的匹配两类方法。由于不同种类传感器的成像原理不同，使得同一场景的多源遥感图像之间灰度相差较大。若匹配时仍采用对灰度相关性要求比较高的归一化互相关系数法，得不到很好的效果，且受噪声的影响很大；若采用基于边缘提取的特征匹配方法，难以同时得到一致的图像边缘和轮廓信息而造成匹配误差，且对水域等均质区域，因其缺少特征使得特征匹配无法进行。

互信息匹配度量自1994年被用于医学图像配准以来，得到了广泛的应用。它不必对不同成像模式下的图像灰度关系作任何假设，且勿需进行预处理，具有精度高、鲁棒性强等特点，非常适合多模态图像匹配。据此人们将其应用于多源遥感图像匹配中。如Cole-Rhodes等(2003)研究了一种基于随机梯度和互信息测度的匹配算法，实验证明了互信息比互相关更适于多源图像匹配。田伟刚等(2008)采用区域互信息作为相似性度量准则，解决了谱间灰度相关性较弱的问题。然而互信息度量用于图像匹配时，其匹配精度有待进一步提高；且匹配过程中需要以穷举方式计算互信息，耗时较多，降低了匹配的实时性。

针对匹配精度问题，考虑在图像匹配中引入基于Tsallis熵(Furuichi, 2006; Martin 等, 2001; Waleed & Ben, 2009)的互信息。传统的Shannon信息熵描述的系统是广度的(可加的)，而实际的系统或多或少地具有时间和空间上的相关性，即非广度性。Tsallis提出了非广度熵测度，即Tsallis熵，与Shannon熵相比具有普适性，且更为准确有效。在图像匹配中，采用基于Tsallis熵的互信息取代基于Shannon熵的互信息作为相似性度量准则，以期进一步提高匹配精度。

针对匹配算法的运算效率问题，近年来提出改进的匹配算法。这些算法或者通过缩小搜索空间减少计算量，如借助小波变换的多分辨率特性，由粗到细逐层匹配(You & Bhattacharya, 2000; Yutaro等,

收稿日期: 2009-07-23; 修订日期: 2009-11-09

基金项目: 国家自然科学基金资助项目“The National Natural Science Foundation of China”资助(No.60872065)。

第一作者简介：吴一全(1963—), 男, 博士, 教授, 信息与通信工程专业, 研究方向为图像处理、分析与理解, 目标检测与跟踪, 信号处理等。已在核心期刊和国际学术会议论文集发表学术论文 90 余篇。E-mail: nuaaimage@yahoo.com.cn。

2007); 或者采用各种优化算法(Chalermwat 等, 2001; 杨帆 & 张汗灵, 2006; 张倩等, 2008; 徐建斌等, 2005), 其中最典型的是遗传算法, 通过非遍历寻优搜索策略加快匹配速度。近年提出的Contourlet变换(Donoho & Vetterli, 2005)具有多分辨率、局部定位、多方向性、近邻界采样和各向异性等优良性质。因此在图像匹配中同样可以考虑利用Contourlet变换的多分辨率等有关特性。后者常用的遗传算法局部寻优能力较差, 参数选择对结果影响大。而粒子群优化算法(Particle Swarm Optimization, PSO)(Sjahputera & Keller, 2005; Li & Ji, 2007)通过群体中粒子的学习与更新实现群体智能优化搜索。与遗传算法相比, 简单、易实现, 需调整的参数少, 是一种高效的并行搜索算法。利用PSO来搜索最佳匹配点, 可大大减少运算时间。

鉴于上述原因, 本文提出了一种基于Contourlet变换、Tsallis熵和改进粒子群的多源遥感图像匹配算法。该算法主要包含以下3个方面: (1)将目标图像和参考图像进行Contourlet分解, 在低分辨率图像进行粗匹配; 根据粗匹配结果在高分辨率下进一步匹配; 最终实现全分辨率情况下遥感图像的匹配。(2)针对目标图像与参考图像中相同大小的子图像, 引入基于Tsallis熵的互信息作为相似性度量, 从而提高匹配精度。(3)在匹配时, 利用一种改进的带极值扰动的简化粒子群优化算法来搜索最佳匹配位置, 进一步提高运算速度。

2　Contourlet 变换、粒子群和互信息的基本原理

2.1　Contourlet 变换

离散 Contourlet 变换也称塔形方向滤波器组(Pyramidal Direction Filter Bank, PDFB), 它由子带分解和方向变换两个步骤实现。首先用拉普拉斯塔形滤波器结构对图像进行多尺度分解, 以“捕获”奇异点; 然后由方向滤波器组将分布在同方向上的奇异点合成为一个系数。图 1 给出了 Contourlet 变换的滤波器组结构, 原始图像经 Contourlet 分解, 得到低通图像和分布于多尺度多方向上的高频分量。

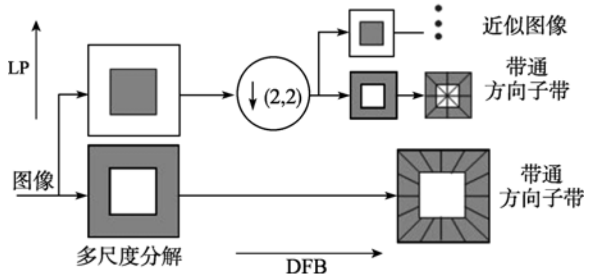

图 1　Contourlet 变换的滤波器组

2.2　基本粒子群优化算法(bPSO)

设在n维搜索空间中, 每个粒子i有位置$\boldsymbol{X}_i=(X_{i1},X_{i2},\cdots,X_{in})$和速度$\boldsymbol{V}_i=(V_{i1},V_{i2},\cdots,V_{in})$, 前者表示问题的解, 对应的目标函数值作为评价该粒子优劣程度的适应度; 后者表示粒子从当前位置移动到下一个位置的速度。首先初始化粒子群, 然后通过迭代方式寻找最优解。假设在第t次迭代时刻, 粒子i的最优解为$\boldsymbol{p}_i(t)$, 称为个体极值, 整个粒子群当前所找到的最优解为$\boldsymbol{g}(t)$, 称为全局极值。在t+1次迭代时刻, 粒子i按下式更新其速度和位置:

$$\begin{aligned}\boldsymbol{V}_i(t+1)=w\boldsymbol{V}_i(t)+c_1r_1\left[\boldsymbol{p}_i(t)-\boldsymbol{X}_i(t)\right]+\\ c_2r_2\left[\boldsymbol{g}(t)-\boldsymbol{X}_i(t)\right]\end{aligned}\tag{1}$$

$$\boldsymbol{X}_i(t+1)=\boldsymbol{X}_i(t)+\boldsymbol{V}_i(t+1)\tag{2}$$

式中: 学习因子 $c_1=c_2=2$; r_1、r_2是均匀分布在(0,1)上的随机数; w是惯性因子, 一般设为随迭代次数t线性递减, 即

$$w=w_{\max}-t\times\frac{w_{\max}-w_{\min}}{t_{\max}}\tag{3}$$

式中, $w_{\max}$和$w_{\min}$分别表示最大和最小惯性因子, $t_{\max}$表示总的迭代次数。在迭代更新过程中,粒子每一维的速率限制成$V_i\in[V_{\min}, V_{\max}]$, 位置限制在允许范围之内, 最后输出的$\boldsymbol{g}$为全局最优解。

2.3　基于 Shannon 熵的互信息

互信息通常用于描述两个系统间的统计相关性, 它可以用熵来表示。系统A的Shannon熵定义

$$H(A)=-\sum_a p_A(a)\log p_A(a)\tag{4}$$

两个系统 A 和 B 的联合熵

$$H(A,B)=-\sum_{a,b}p_{A,B}(a,b)\log p_{A,B}(a,b)\tag{5}$$

式中, $a\in A$, $b\in B$; $p_A(a)$表示系统 A 的概率密度; $P_{A,B}(a,b)$表示系统A、B的联合概率密度。如果$H(A|B)$表示已知系统B时A的条件熵, 那么两个系统的互信息可描述

$$\begin{aligned}I(A,B)&=H(A)+H(B)-H(A,B)\\&=H(A)-H(A\mid B)\end{aligned}\tag{6}$$

采用概率分布之间的广义距离来估计互信息

$$I(A,B)=\sum_{a,b}p_{A,B}(a,b)\log\frac{p_{A,B}(a,b)}{p_A(a)p_B(b)}\tag{7}$$

3　多源遥感图像匹配算法实现过程

提出一种基于Contourlet变换、Tsallis熵和改进

粒子群的多源遥感图像匹配算法。该算法利用Contourlet变换的多分辨率特性，由粗到细逐层匹配；引入基于Tsallis熵的互信息作为相似性度量准则以提高匹配精度；同时采用一种改进的带极值扰动的简化粒子群优化算法(mtsPSO)，改善基本粒子群优化算法(bPSO)在搜索过程中易陷入局部极值、后期收敛速度慢和精度低的情况。上述多源遥感图像匹配算法的具体实现过程如下:

(1) 对目标图像和参考图像分别进行Contourlet变换，得到两组Contourlet分解系数。其中，LP采用“9-7”金字塔滤波器，其原因是线性相位并且近似满足正交性的特点使得“9-7”滤波器更适合于图像信号的处理。DFB采用“pkva”方向性滤波器，每层都分解为4个方向。分解层数L由目标图像决定，分解后低频图像不应太小，否则会因所含信息太少易造成误匹配，本文取L=2。

(2) 在参考图像的低频部分初始化粒子群：随机生成m个粒子的位置$\boldsymbol{X}$，$\boldsymbol{X}$为目标图像相对参考图像的位置偏移量(Δx，Δy)，每个粒子的$\boldsymbol{p}$设置为其当前位置，$\boldsymbol{g}$设置为任意一个粒子的$\boldsymbol{p}$。设置参数：$t_{\max}$=500, t=0, m=50。

(3) 计算适应度函数。考虑目标图像A与参考图像中相同大小的子图像B，以其基于Tsallis熵的互信息$I_q(A，B)$作为适应度函数，由粒子位置$\boldsymbol{X}$求各粒子的适应度F_p，下面给出推导过程。

对于任意非负实数q和任意给定的变量x的概率分布$p(x)$, Tsallis熵定义为

$$S_q(X)=\frac{1}{q-1}\left[1-\sum_x p(x)^q\right] \tag{8}$$

特别地，当$q\to 1$时, Tsallis熵收敛于Shannon熵。

基于Tsallis熵的互信息公式推导如下:

$$\begin{aligned} I_q(A,B)&=S_q(A)-S_q(A|B)\\ &=S_q(A)+S_q(B)-S_q(A,B)\\ &=S_q(A)+S_q(B)-[S_q(A)+S_q(B)+\\ &\quad (1-q)S_q(A)S_q(B)]\\ &=(q-1)S_q(A)S_q(B) \end{aligned} \tag{9}$$

将式(8)代入，得

$$\begin{aligned} I_q(A,B)=\frac{1}{|q-1|}[1-\sum_a p(a)-\sum_b p(b)+\\ \sum_a p(a)\sum_b p(b)] \end{aligned} \tag{10}$$

在多源遥感图像匹配问题中，虽然目标图像和参考图像来源于不同的成像设备，但是它们基于同一场景，当目标图像和参考图像中相同大小的子图像完全匹配时，其中一幅图像中表达的关于另一幅图像的信息，即对应像元的互信息应为最大。

(4) 更新个体极值$\boldsymbol{p}$、全局极值$\boldsymbol{g}$。如果粒子的适应度优于该粒子当前个体极值对应的适应度，则将$\boldsymbol{p}$设置为该粒子的位置，更新个体极值；如果所有粒子的最佳个体极值对应的适应度优于当前全局极值对应的适应度，则将$\boldsymbol{g}$设置为该粒子的位置，更新全局极值。

(5) 根据粒子状态更新粒子 $\boldsymbol{X}$。mtsPSO 算法去掉了 bPSO 进化方程的粒子速度项而使原来的二阶微分方程简化为一阶微分方程，仅由粒子位置控制进化过程，避免了由粒子速度项引起的粒子发散而导致后期收敛速度变慢和精度低的问题，同时通过增加极值扰动算子加快粒子跳出局部极值点而继续优化，从而使粒子群优化算法更为实用。mtsPSO 算法中粒子的更新过程为

$$\begin{aligned} \boldsymbol{X}_i(t+1)=w\boldsymbol{X}_i(t)+c_1r_1[r_3^{t_0>T_0}p_i-\boldsymbol{X}_i(t)]\ +\\ c_2r_2[r_4^{t_g>T_g}g-\boldsymbol{X}_i(t)] \end{aligned} \tag{11}$$

式中：t_0，t_g 分别表示个体极值和全局极值进化停滞步数；T_0，T_g 表示个体极值和全局极值需要扰动的停滞步数阈值；

$r_3^{t_0>T_0}=\begin{cases}1 & t_0\leqslant T_0\\ U(0,1) & t_0>T_0\end{cases}$ 和 $r_4^{t_g>T_g}=\begin{cases}1 & t_g\leqslant T_g\\ U(0,1) & t_g>T_g\end{cases}$ 表示带条件的均匀随机数，$U(0,1)$表示均匀分布在 (0,1) 上的随机数。本文取 $T_0=T_g=10$。

考虑到较大的惯性权重因子有利于提高算法的全局搜索能力，较小的惯性权值可增强算法的局部能力，本文的 mtsPSO 算法对带极值扰动简化粒子群优化算法(胡望 & 李志蜀，2007)作了修改，采用下列惯性权值递减策略(陈贵敏等，2006)，使其自适应达到最佳平衡惯性因子，如下式(12):

$$\begin{aligned} w=(w_{\text{start}}-w_{\text{end}})\left(\frac{t}{t_{\max}}\right)^2+\\ (w_{\text{end}}-w_{\text{start}})\left(\frac{2t}{t_{\max}}\right)+w_{\text{start}} \end{aligned} \tag{12}$$

本文取 $w_{\text{start}}=0.95, w_{\text{end}}=0.4$。

(6) 迭代：令t=t+1。检验是否符合结束条件：如果当前的迭代次数达到预先设定的最大次数$t_{\max}$或满足给定精度则停止迭代，输出最优解，否则转到步骤(3)。

(7) 根据迭代后最优解所在的位置$\boldsymbol{g}_L$，输出低频部分的最佳偏移位置Δx_L、Δy_L。

(8) 在尺度L–1上，以$2\Delta x_L$、$2\Delta y_L$为中心的邻域内继续搜索，找到该层的最佳偏移位置Δx_{L-1}、Δy_{L-1}。

重复这个过程，直至最终找到全分辨率下的最佳偏移位置Δx_0、Δy_0。

4 实验结果与分析

针对200组遥感图像进行了实验，现选取其中3组遥感图像加以说明，分别是256×256的SPOT图像(图2(a))与50×50的TM图像(图2(b))；256×256的可见光图像(图2(d))与50×50的SAR图像(图2(e))；256×256的可见光图像(图2(g))与50×50的红外图像(图2(h))。采用本文提出的基于Contourlet域Tsallis熵和带极值扰动的简化粒子群的图像匹配算法，在Intel Pentium4 2.78GHz CPU、512M内存、MATLAB 7.1环境中运行，匹配结果如图2(c), (f), (i)所示。

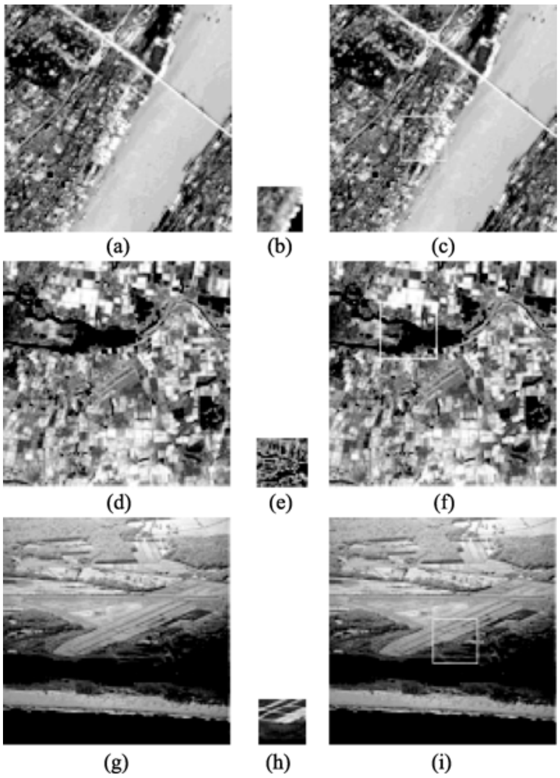

图2 3组实验图像

(a) 实验1的参考图像；(b) 目标图像；(c)匹配结果；(d) 实验2的参考图像；(e) 目标图像；(f) 匹配结果；(g) 实验3的参考图像；(h) 目标图像；(i)匹配结果

4.1 取不同分解层 *L* 的实验结果比较

分解层L的取值应该由目标图像的大小决定。分别对以上3组遥感图像进行实验，程序运行50次，匹配位置取其平均值，结果如表1。表1中给出的坐标均为匹配位置左上角坐标。

表1 取不同分解层时的匹配结果

	分解层 L	匹配位置	匹配误差	平均时间/s
实验1	0	(122,80)	(−4, −2)	10.47238
	1	(126,82)	(0,0)	5.99021
	2	(126,82)	(0,0)	3.38824
实验2	0	(37,46)	(0,0)	10.01475
	1	(37,46)	(0,0)	5.78250
	2	(37,46)	(0,0)	3.22392
实验3	0	(114,120)	(−1,2)	10.75026
	1	(115,118)	(0,0)	6.10187
	2	(115,118)	(0,0)	3.40373

由表1看出，当L取的值偏小时，有较小的匹配误差，且耗时较长；L越大，耗时越少，但当L偏大时，由于分解层数变多，低频部分信息量变少，易造成误匹配。

4.2 不同方法的实验结果比较

为了便于比较，采用了以下几种常见的匹配算法对实验图像进行匹配：(a)基于互相关和PSO的图像匹配算法(Sjahputera & Keller, 2005)；(b)基于互信息和PSO的图像匹配算法(Li & Ji, 2007)；(c)基于小波变换、互信息和遗传算法的图像匹配算法(杨帆 & 张汗灵, 2006)；(d)基于小波变换、互信息和PSO的图像匹配算法(张倩等，2008)；(e)本文提出的基于Contourlet变换、Tsallis熵和mtsPSO的图像匹配算法。其中分解层数取L=2, q=0.8，每种算法重复运行50次，当匹配误差为(0,0)时认为解正确，上述不同算法的匹配结果比较如表2所示，其中匹配正确率定义为匹配正确次数与算法重复运行的总次数之比。

表2 不同算法的匹配结果

	匹配算法	平均时间/s	正确率/%
实验1	(a)	4.99721	0
	(b)	50.01207	8
	(c)	19.38394	46
	(d)	14.14857	42
	(e)	3.38824	92
实验2	(a)	4.68990	2
	(b)	50.92149	10
	(c)	19.28786	60
	(d)	14.87391	60
	(e)	3.22392	98
实验3	(a)	4.66313	0
	(b)	50.69498	6
	(c)	18.85430	40
	(d)	14.00925	38
	(e)	3.40373	96

由于遗传算法、粒子群算法等这些寻优算法所求得的解具有一定的不确定性，多次运行程序可以发现：算法(a)正确次数几乎为零，这是因为SAR、红外和可见光等遥感图像的成像原理不同，使得图像之间灰度相差很大，在这种情况下，图像的灰度线性关系不成立，利用传统的互相关不能搜索到精确的匹配点。相比算法(a)，算法(b)采用互信息作为相似性度量准则，一定程度上克服了灰度引起的误匹配，但由于搜索范围较大，PSO的参数相对设置较高，计算量仍然偏大。算法(c)、算法(d)在算法(b)的基础上引入了小波变换，在保证正确率的同时，速度明显提高，其中算法(c)的耗时相对较长，这是因为遗传算法较粒子群算法多了交叉、变异等步骤，因此运行速度较算法(d)慢。算法(e)采用基于Contourlet变换、Tsallis熵互信息和mtsPSO的匹配算法，精确度明显大于其他4种算法，稳定性最好，且计算速度较算法(b) (c) (d)快4倍以上。

4.3　算法的抗噪性能

在给出的3组实验图像中加入均值为0，方差为0.01 的高斯噪声，利用本文提出的算法进行匹配，结果如图 3。

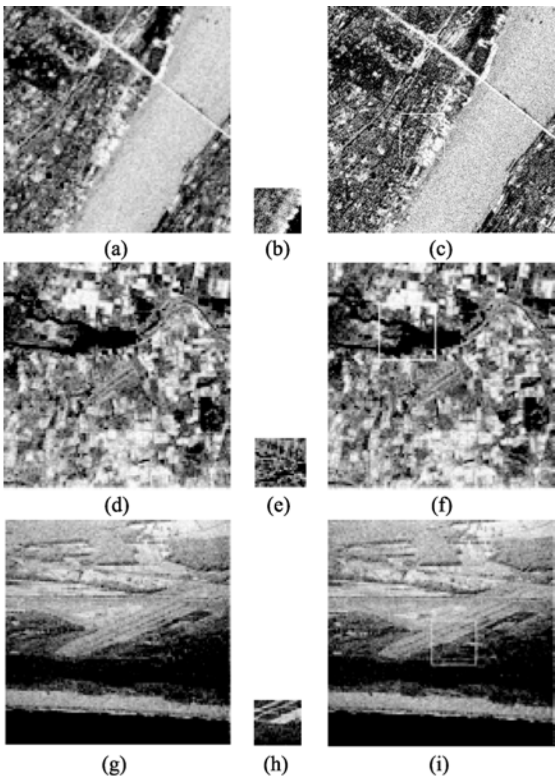

图 3　3 组加噪的实验图像

(a) 实验 1 的参考图像; (b) 目标图像; (c) 匹配结果; (d) 实验 2 的参考图像; (e) 目标图像; (f) 匹配结果; (g) 实验 3 的参考图像; (h) 目标图像; (i) 匹配结果

进行了多次实验，匹配结果分别为(126, 80)、(38, 46)、(115, 118)，匹配误差分别为(0,–2)、(1,0)、(0,0)。可以看出，采用本文提出的算法对带噪声的图像进行匹配时，仍能得到较为准确的匹配结果，算法具有一定的抗噪声性能。且经过多次实验证明，目标图像越大，其对噪声的抑制能力越强。原因是图像越大，参与匹配运算的图像信息量越大，从而增强了算法对噪声的抑制能力。

5　结　论

本文提出了一种基于 Contourlet 变换、Tsallis熵和改进粒子群的遥感图像匹配算法。在对目标图像和参考图像进行 Contourlet 分解的基础上，引入基于 Tsallis 熵的互信息度量准则，利用一种带极值扰动的简化粒子群优化算法对低分辨率的遥感图像进行匹配操作，逐级上推，最终实现全分辨率情况下的多源遥感图像的匹配。实验选取了不同分解层数、不同方法进行比较。结果表明，该算法与目前常用的匹配算法相比，匹配精度和运算效率都有大幅提高，且该算法对噪声具有一定的鲁棒性。下一步工作考虑大角度旋转下的图像匹配问题。

REFERENCES

Barbara Z and Jan F. 2003. Image registration methods: a survey. *Image and Vision Computing*, **21**(11): 977—1000

Brown L G. 1992. A survey of image registration techniques. *ACM Computing Surveys*, **24** (4): 325—376

Chalermwat P, El-Ghazawi T and LeMoigne J. 2001. Two-phase genetic algorithm-based image registration on parallel clusters. *Journal of Future Generation Computing Systems*, **17**: 467—476

Chen G M, Jia J Y and Han Q. 2006. Study on the strategy of decreasing inertia weight in particle swarm optimization algorithm. *Journal of Xi’an Jiaotong University*, **40**(1): 53—56

Cole-Rhodes A A, Johnson K L, Le-Moigne J and Zavorin I. 2003. Multiresolution registration of remote sensing imagery by optimization of mutual information using a stochastic gradient. *Image Processing*, **12**(12): 1495—1511

Donoho M N and Vetterli M. 2005. The contourlet transform: an efficient directional multiresolution image representation. *IEEE Transactions on Image Processing*, **14**(12): 2091—2106

Furuichi S. 2006. Information theoretical properties of tsallis entropies. *Journal of Mathematical Physics*, **47**(2): 23302-1—18

Hu W and Li Z S. 2007. A simpler and more effective particle swarm optimization algorithm. *Journal of Software*, **18**(4): 861—868

Li Q and Ji H B. 2007. Medical image registration based on maximization of mutual information and particle swarm optimization. 5th International Conference on Photonics and Imaging in Biology and Medicine, **6534**: 5342—5344

Li X M, Zheng L and Hu Z Y. 2006. SIFT based automatic registration of remotely-sensed imagery. *Journal of Remote Sensing*, **10**(6): 885—892

Martin S, Morison G H, Nailon W H and Durrani. 2001. Fast and accurate image registration using tsallis entropy and simultaneous perturbation stochastic approximation. *IET Electronics Letters*, **40**(10): 595—597

Sjahputera O and Keller JM. 2005. Particle swarm over scene matching. IEEE Swarm Intelligence Symposium

Tian W G, Guo L, Li H H and Yang W L. 2008. A point-based algorithm for multi-spectral image registration using mutual information of regions. *Journal of Optoelectronics Laser*, **19**(6): 799—783

Waleed M and Ben H A. 2009. Nonextensive entropic image registration. *Image Analysis and Recognition*, **5627**: 116—125

Xu J B, Hong W and Wu Y R. 2005. The study of remote sensing images matching method based on wavelet transform and genetic algorithms. *Journal of Electronics & Information Technology*, **27**(2): 283—285

Yang F and Zhang H L. 2006. Multiresolution 3-D image registration using hybrid genetic algorithm and powell's method. *Journal of Optoelectronics · Laser*, **17**(6): 26—30

You J and Bhattacharya P A. 2000. Wavelet-based coarse-to-fine image matching scheme in a parallel virtual machine environment. *IEEE Transactions on Image Processing*, **9**(9): 1547—1559

Yutaro Y, Hyoungseop K, Jookooi T, Ishikawa S and Yamaoto A. 2007. A method for reducing of computation time on image registration employing wavelet transformation. International Conference on Control, Guangzhou

Zhang J X, Li G S and Zeng Y. 2005. The study on automatic and high-precision rectification and registration of multi-source remote sensing imagery. *Journal of Remote Sensing*, **9**(1): 73—77

Zhang Q, Yang J and Jia D D. 2008. Image registration based on wavelet transform and hybrid optimization algorithm. *Computer Engineering*, **34**(7): 189—191

附中文参考文献

陈贵敏，贾建援，韩琪. 2006. 粒子群优化算法的惯性权值递减策略研究. 西安交通大学学报, **40**(1): 53—56

胡望，李志蜀. 2007. 一种更简化而高效的粒子群优化算法. 软件学报, **18**(4): 861—868

李晓明，郑链，胡占义. 2006. 基于 SIFT 特征的遥感影像自动配准. 遥感学报, **10**(6): 885—892

田伟刚，郭雷，李晖晖，杨卫莉. 2008. 基于区域互信息的特征级多光谱图像配准. 光电子·激光, **19**(6): 799—783

徐建斌，洪文，吴一戎. 2005. 基于小波变换和遗传算法的遥感影像匹配方法的研究. 电子与信息学报, **27**(2): 283—285

杨帆，张汗灵. 2006. 遗传算法和 Powell 法结合的多分辨率的三维图像配准. 光电子·激光, **17**(6):26—30

张继贤，李国胜，曾钰. 2005. 多源遥感影像高精度自动配准的方法研究. 遥感学报, **9**(1): 73—77

张倩，杨静，贾丁丁. 2008. 基于小波变换和混合优化算法的图像配准. 计算机工程, **34**(7): 189—191